NASA TECHNICAL NOTE

NASA TN D-3420

NASA TN D-3420

PHOTOGRAPHIC OBSERVATIONS OF A LOW-DENSITY IRON ARTIFICIAL METEOROID

by Gale A. Harvey

Langley Research Center

Langley Station, Hampton, Va.

NATIONAL AERONAUTICS AND SPACE ADMINISTRATION • WASHINGTON, D. C. • MAY 1966

NASA TN D-3420

PHOTOGRAPHIC OBSERVATIONS OF A LOW-DENSITY IRON ARTIFICIAL METEOROID

By Gale A. Harvey

Langley Research Center
Langley Station, Hampton, Va.

NATIONAL AERONAUTICS AND SPACE ADMINISTRATION

For sale by the Clearinghouse for Federal Scientific and Technical Information
Springfield, Virginia 22151 – Price $1.00

PHOTOGRAPHIC OBSERVATIONS OF A LOW-DENSITY IRON ARTIFICIAL METEOROID

By Gale A. Harvey
Langley Research Center

SUMMARY

A shaped charge, boosted to an altitude of 48 kilometers by a single-stage rocket, was used to accelerate 1.5 grams of minute cast-iron particles to a velocity in excess of 10 kilometers per second. The radiation from this artificial meteor was measured with ballistic cameras and modified aerial cameras using panchromatic film. A light curve was established, and a spectrum of the event was analyzed.

The first half of the short meteor trail was masked by the explosion of the shaped charge, and, thus, the radiation from the iron dust ball was only measured for that portion of the trail, about 100 meters long, outside the fireball of the explosion. The maximum measured light intensity of the meteor was -0.4 of an absolute meteor magnitude as determined by use of intensity of background stars for calibration. A lower limit of 0.95×10^{-3} was obtained for the luminous efficiency factor for panchromatic film. Calculations indicate that if the low-density iron meteor had been produced at an altitude of 70 kilometers, the intensity would be 3 magnitudes less than at 48 kilometers but still bright enough to be recorded by optical systems similar to those used for natural meteor detection.

A spectrum of the meteor was measured with a K-24 aerial camera equipped with an objective diffraction grating. Some 200 lines and 35 multiplets of iron were identified in a wavelength reduction of the spectrum. A trace of the cast-iron liner impurity (manganese) was observed in the spectrum. The aluminum case around the shaped charge did not contaminate the meteor trail, and the sodium D lines generally seen in natural meteor spectra were not identified.

INTRODUCTION

A basic constraint in the theory of meteors is the inability to measure the physical characteristics of a meteoroid prior to its capture by the earth's atmosphere. The mass, composition, and the density of the meteoroid are all unknown. The classical theory, together with the measured observables of natural meteors, can at best only postulate these parameters within relatively broad limits. (See refs. 1 and 2.) The limits are too

large for engineering applications, especially in the design of meteoroid shields for spacecraft. However, if the mass, composition, and density of a meteoroid are known prior to its entry into the earth's atmosphere, it is then feasible to determine two unresolved and basic coefficients employed in the physical theory of meteors; namely, the luminous efficiency and the ionization efficiency. The luminous efficiency is the ratio of the light energy radiated from the meteor to the kinetic energy of the meteoroid. Similarly, the ionization efficiency is the ratio of the ionization energy to the kinetic energy of the meteoroid. A more complete discussion of the subject may be found in reference 2.

A Meteor Simulation Project has been established by NASA with the objective of determining the luminous and ionization efficiencies of some of the more predominant materials known to exist in natural meteors. Artificial meteoroids, of known mass, composition, and density, are reentered into the earth's atmosphere at low meteoric speeds by means of simple rocket vehicles and shaped-charge accelerators. Optical and radar measurements are made, with equipment similar to that used in natural meteor detection, to provide a calibration of the accumulated data on natural meteors. The feasibility of producing an artificial meteor in a controlled experiment has been demonstrated in other flight projects. (See refs. 3, 4, and 5.)

The research presented in this paper was conducted as an early part of the Meteor Simulation Project for the following purposes:

(1) to evaluate the performance of a particular shaped-charge accelerator, or gun, under flight conditions

(2) to appraise the optical instrumentation planned for use in future artificial meteor tests

(3) to obtain the spectra of a low-density, iron, artificial meteor

(4) to obtain a preliminary value of the luminous efficiency of a low-density iron artificial meteor

The vehicle used in this test was one of four Arcas-Margo vehicles donated to the NASA by the Office of Naval Research. The Physical Science Laboratory of New Mexico State University developed the Margo payload, and the Ballistic Research Laboratories at Aberdeen Proving Ground developed the shaped-charge accelerator. The test was performed at Wallops Island, Va., on September 26, 1963.

Whipple in reference 6 and Öpik in reference 1 contend that most meteors are composed of a large number of minute particles; these meteoroids are often classified as dust balls. The first known artificial meteor was produced in 1957 at White Sands, New Mexico, by use of an Aerobee rocket and shaped charges that produced aluminum dust balls. From this test, McCrosky (ref. 5) derived a lower limit for the luminous

efficiency of natural meteoric material by assuming equal efficiencies, per atom, of iron and aluminum. Natural meteoroids contain from 15 percent to more than 90 percent iron, and a test of an iron dust ball would therefore provide a more direct calibration of natural meteors. However, it was first necessary to determine whether an iron dust ball could be produced at natural meteor altitudes; secondly, it was imperative to know whether this particular artificial meteor would be bright enough to be detected by spectral and streak cameras. (See table I.) This information was necessary in order to plan effectively for the types of payloads to be employed in the more advanced vehicles of the Meteor Simulation Project. However, some compromises had to be made. The thrust impulse of the Arcas vehicle restricted its peak altitude to about 50 kilometers, whereas natural meteors become visible between altitudes of 70 and 100 kilometers. At 50 kilometers the blast of the gun masks about half of the meteor trails. The length of the trail is about 1/50 of that for a natural meteor. Because of the short duration of this artificial meteor, its velocity had to be determined from preflight ballistic tests rather than from measurements in flight. Thus, the calculated value of the luminous efficiency is conditioned on these restrictions, but since these are the first data on a low-density, iron artificial meteor, a lower limit of the luminous efficiency has been presented.

TABLE I.- LIMITS OF CAMERA DETECTIVITY

[Values are in absolute meteor magnitudes]

	Meteor camera Super Schmidt	Ballistic 210-mm camera	K-24	Modified 610-mm aerial camera
Undispersed	+5	+2	+2	0
Spectrally dispersed	+1	---	-2	---

FLIGHT VEHICLE AND SHAPED-CHARGE ACCELERATOR

The flight vehicle is a single-stage, end-burning, solid-propellant Arcas booster having a nominal thrusting time of 28 seconds and a Margo payload. The geometry and pertinent dimensions of this vehicle are shown in figure 1. The Arcas used weighed 30 kilograms before launch and carried a total payload weight of 5.5 kilograms.

The Margo (figs. 2 and 3) includes the nose cone, shaped-charge accelerator, batteries, timer, and parachute. A photograph and a sketch of the shaped-charge accelerator are shown as figure 4. The shaped-charge accelerator was encased in a thick-wall aluminum cylinder 9.9 centimeters in diameter and 20.2 centimeters long. About 1.8 kilograms of explosive, composed of 50 percent pentolite and 50 percent TNT, was cast in the aluminum cylinder around a 20^{o} conical liner of meehanite cast iron. A shock-type detonator, fired by a preset timer using a battery-powered electrical circuit, caused the charge to explode. The pressure from this explosion collapsed the cast-iron liner and accelerated a small part of the liner to a velocity in excess of 10 kilometers per second. Most of the liner material trailed the high-speed cloud of iron particles at a velocity of less than 2 kilometers per second.

The velocity and mass of the dust ball of similar accelerators were measured from accurately timed flash X-ray photographs taken in an atmospheric ground range at the Ballistic Research Laboratories, Aberdeen Proving Ground. Figure 5 is a series of three of these flash X-ray photographs. The expelled cast iron at 103 and 156 microseconds after detonation of the shaped-charge accelerator is shown in figures 5(a) and 5(b), respectively. The photograph taken at 184 microseconds after detonation shows decelerating particles trailing after the main body of cast-iron particles (fig. 5(c)). The mass and velocity of the main body of particles determined by the Ballistic Research Laboratories were 1.5 ± 0.5 grams and 10.4 ± 0.4 kilometers per second, respectively. The density of the main body of particles, calculated from the mass and scaled cross section of the X-ray photographs in figures 5(a) and 5(b), were approximately 0.08 and 0.04 gram per cubic centimeter, respectively. McKinley (ref. 2) estimates that the effective density of a natural

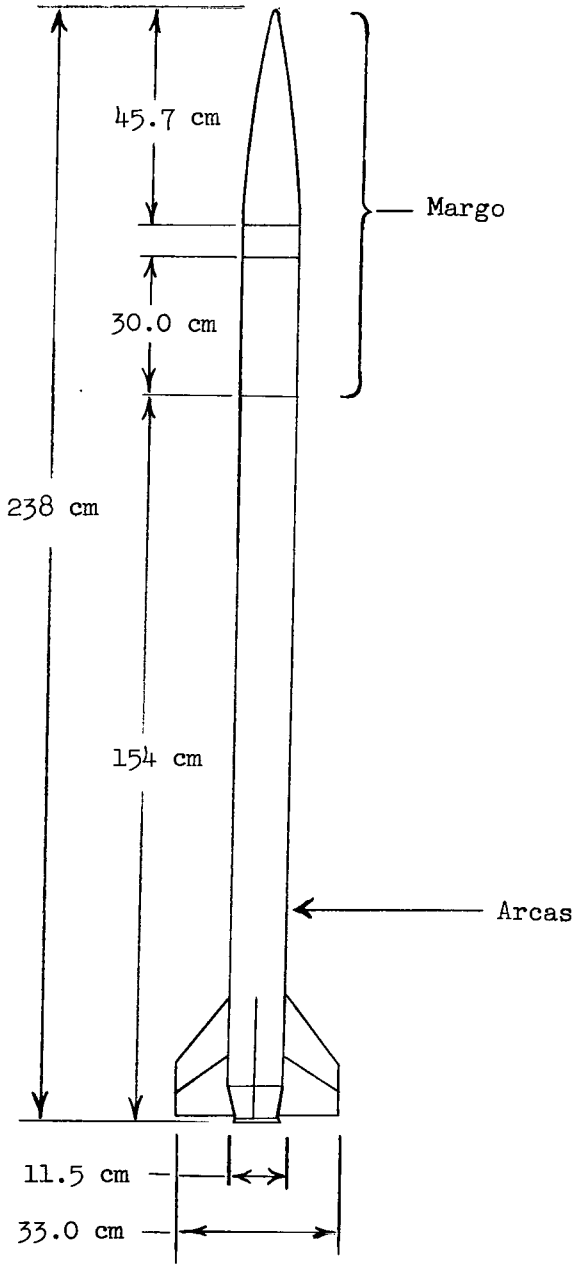

Figure 1.- Arcas-Margo vehicle.

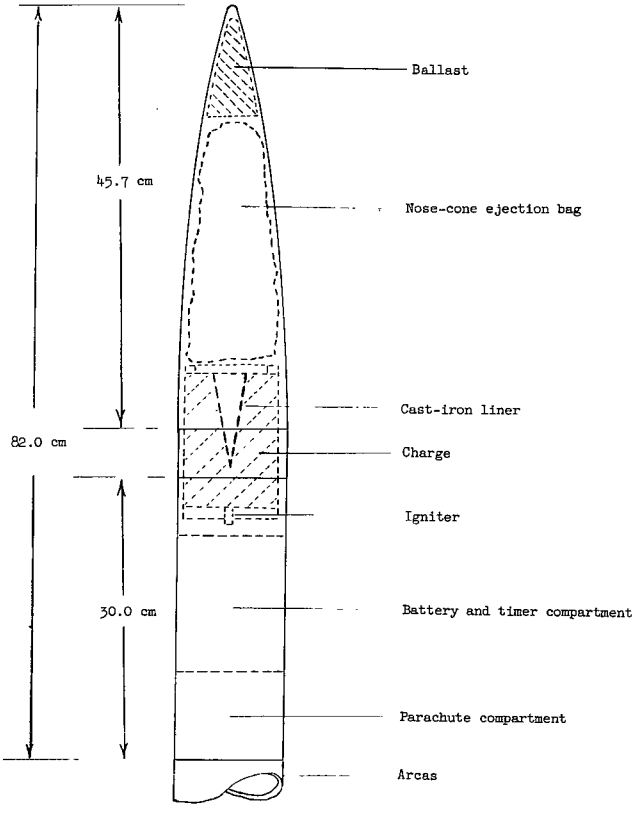

Figure 2.- Margo section.

dust-ball meteoroid may be of the order of 0.05 to 0.5 gram per cubic centimeter. Since the density of the cast-iron liner was 7.8 grams per cubic centimeter, it is apparent that the high-velocity body of iron accelerated from the shaped-charge accelerator was truly a dust ball rather than a solid slug or a jet.

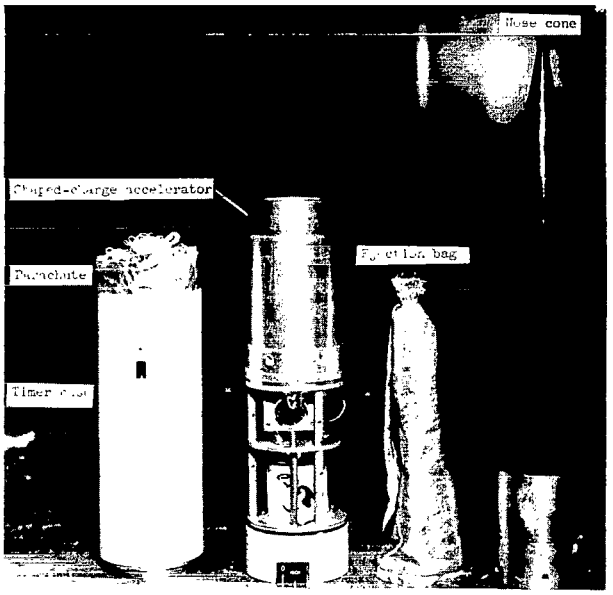

Figure 3.- Margo components. L-63-4829.1

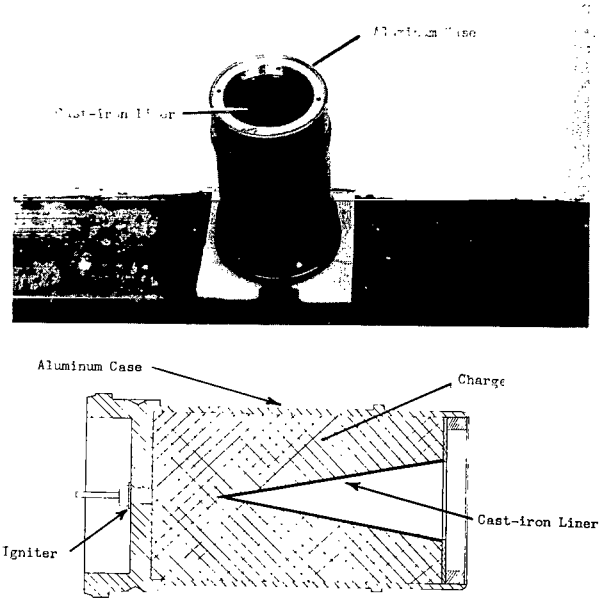

L-64-4705

Figure 4.- Shaped-charge accelerator.

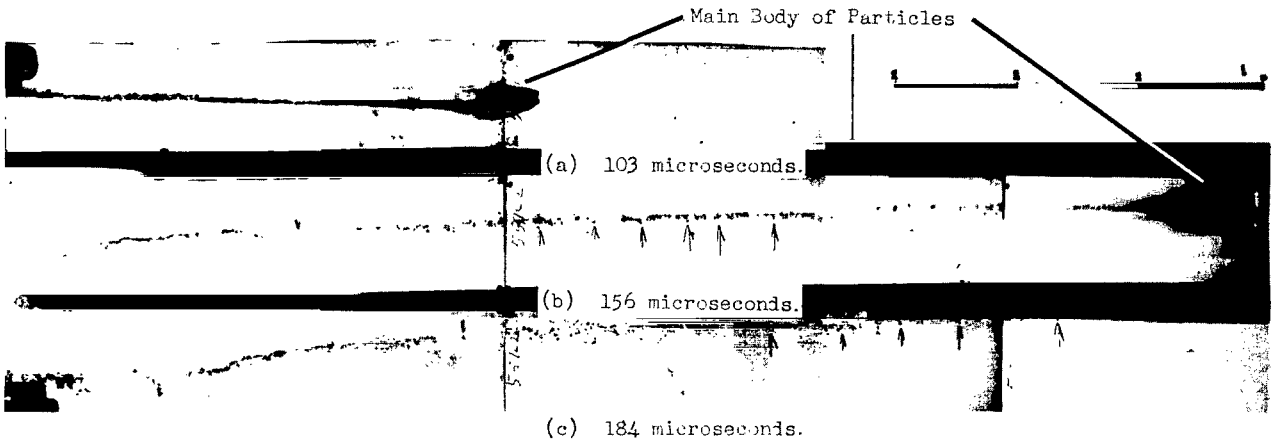

L-64-4706

Figure 5.- Flash X-rays of particles from a shaped-charge accelerator lined with cast iron from Ballistic Research Laboratories ground tests.

FLIGHT TEST

The Arcas-Margo was launched at an azimuth of 154° and an elevation of 83° on a clear, moonless night. The vehicle obtained an altitude of 50 kilometers at which height the nose cone was ejected by a pressurized bag, and the shaped-charge accelerator with a 1-meter parachute was released from the payload package. The parachute was employed to orient the shaped-charge accelerator in a downward direction. The shaped-charge accelerator was detonated at 48 kilometers; figure 6 shows the measured radar trajectory up to detonation of the shaped charge.

The shaped-charge accelerator successfully produced an artificial meteor that was photographed with fixed ballistic cameras and modified aerial cameras, some equipped with objective diffraction gratings. The photographs were taken from two ground-based camera stations located at Wallops Island, Va., and at Sandbridge, Va. The negatives from a ballistic camera (designated BC-4) (210-mm focal length and f/4.2), and from a modified aerial camera (610-mm focal length and f/3.5) were used to obtain photometric intensity data of the artificial meteor. Some ballistic cameras were equipped with an occulting shutter (fig. 7) to measure velocity of reentry trails. This shutter opens and closes 10 times per second. A spectrum was obtained from a modified K-24 aerial camera (178-mm focal length and f/2.5) equipped with a 400-line-per-millimeter objective diffraction grating.

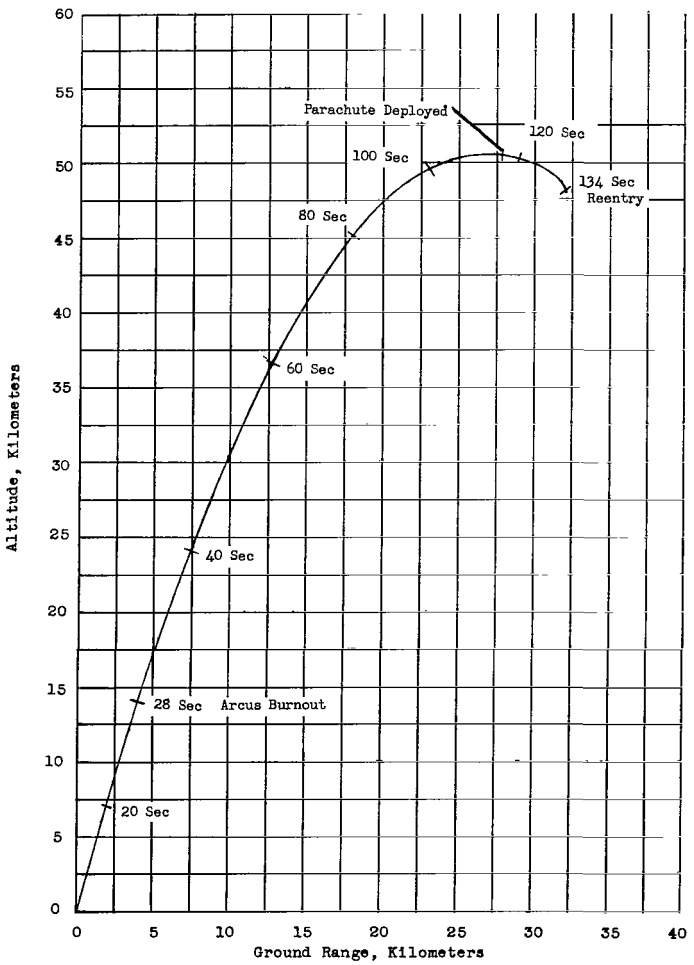

Figure 6.- Trajectory profile (from radar data).

DATA REDUCTION

Determination of the luminous intensity of the artificial meteor was accomplished through the calibration provided by the background stars that were photographed on the same negative as the reentry trail. The photographic densities of the star images and the reentry image were measured

with a microdensitometer. Some 25 to 30 stars of known magnitude were identified to provide a calibration between the photographic density and the light intensity. The star images chosen were about the same angular distance from the optical axis of the camera as the reentry streak and were near the reentry image to minimize the intensity corrections used in the calibration. The visual stellar magnitudes of these calibration stars, as published in reference 7, were then normalized to the optical path of the reentry radiation by correcting each star for the difference in the off-axis light losses through the camera and the difference in the atmospheric absorption. The differences between the trailing velocities of all of the star images were not great enough to be included in the calibration. In general, the total correction to the star intensity was about ±0.6 magnitude but never exceeded ±1.5 magnitudes for any individual star.

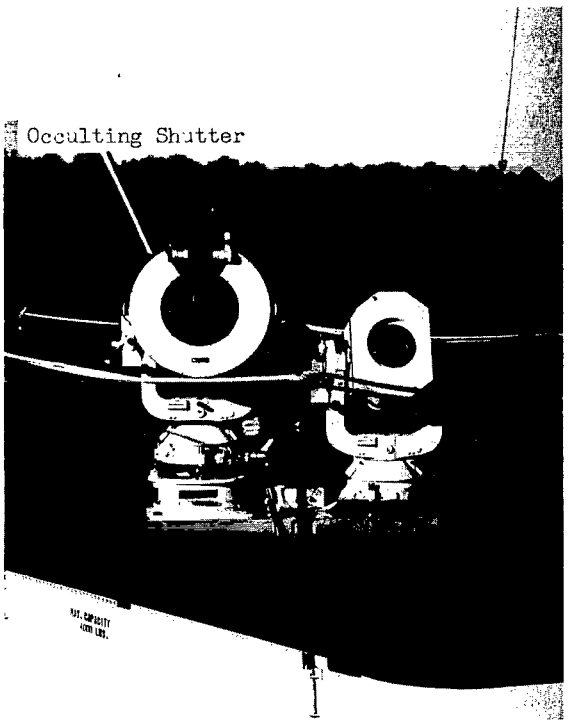

L-61-8237
Figure 7.- The 210-mm focal length f/4.2 cameras.

The apparent stellar intensity of the artificial meteor was determined from the measured density of the photographic image and the star calibration data. However, since the image of the meteor moves across the photographic emulsion much faster than the image of a calibration star, a large correction to the apparent intensity of the meteor was made to account for this difference. The actual intensity of the meteor was -6.73 magnitudes brighter than its apparent stellar photographic intensity. A reciprocity failure correction of 1.15 magnitudes, obtained by the method of reference 8, was applied. Generally the irradiance of a meteor is expressed in terms of an absolute meteor magnitude by normalizing its stellar magnitude to 100 kilometers. The slant range from the camera to the reentry, as obtained from a two-station optical reduction similar to the method used by Whipple and Jacchia in reference 9, was 60 kilometers. A normalizing factor of ±1.18 magnitudes was used to express the intensity in absolute meteor magnitudes.

The identification of the prominent iron lines was made by comparing densitometer tracings of the spectrum with the iron spectra of reference 10. The identified lines were then checked with the wavelength and intensity values given in reference 11.

RESULTS AND DISCUSSION

The observable part of the trail of the artificial meteor was very short, as can be seen from figure 8, which is an enlargement of the reentry photograph from the ballistic camera. The meteor trail, the light from the detonation, and neighboring star trails are present in the photograph. The shape of the image from the detonation light is a result of the camera aberrations.

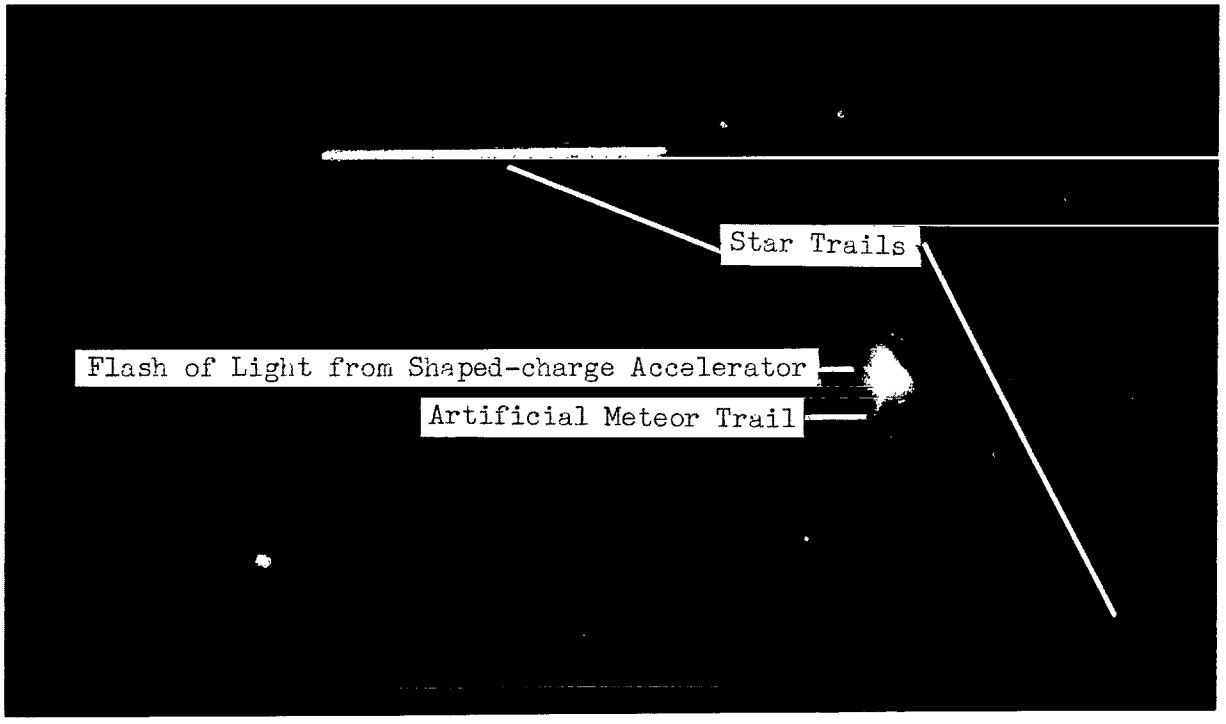

Figure 8.- Enlargement of ballistic-camera photograph of artificial meteor. L-64-4707

The photographic meteoroid trail was very short for several reasons. Approximately one-half of the trail was masked by the flash of light from the detonation of the shaped-charge accelerator. Also, the shaped-charge accelerator was well within the atmosphere when it was ignited at an altitude of 48 kilometers. The relatively dense atmosphere caused a much shorter trail than would be expected of a natural meteor of the same speed that becomes visible at an altitude of 70 kilometers. However, the intensity of the radiation is much greater at an altitude of 48 kilometers than it would be at 70 kilometers. From reference 2 the relation between radiation intensity and altitude, or atmospheric density, can be seen by combining the differential mass equation

$$\frac{dm}{dt} = -\frac{\Lambda A}{2\zeta}\left(\frac{m}{\rho_m}\right)^{2/3}\rho_a V^3 \qquad (1)$$

with the luminous efficiency equation

$$I = -\frac{1}{2}\tau\frac{dm}{dt}V^2 \tag{2}$$

to obtain the luminosity equation

$$I = \tau\frac{\Lambda A}{4\zeta}\left(\frac{m}{\rho_m}\right)^{2/3}\rho_a V^5 \tag{3}$$

where

I	instantaneous radiation intensity (panchromatic film)
τ	luminous efficiency (panchromatic film)
Λ	heat-transfer coefficient
ζ	heat of ablation
$A\left(\frac{m}{\rho_m}\right)^{2/3}$	effective cross-sectional area of body
m	mass of body
ρ_m	density of body
ρ_a	atmospheric density
V	velocity
t	time

The altitude dependence is seen to result from the atmospheric density factor ρ_a. The expression relating magnitude to intensity is

$$M_1 - M_2 = -2.5 \log\frac{I_1}{I_2} \tag{4}$$

where $M_1 - M_2$ is the magnitude difference between the two intensities I_1 and I_2. By use of equations (3) and (4) and values of atmospheric density from reference 12, the maximum intensity of a meteor at a 70-kilometer altitude is calculated to be 3 magnitudes less than that of a meteor at a 48-kilometer altitude if other parameters are held constant.

An artificial low-density iron meteor at 70 kilometers would be approximately zero absolute meteor magnitudes in brightness and the undispersed optical instrumentation used in this experiment (table I) would be capable of recording the meteor. Modified aerial cameras with objective diffraction gratings would not be capable of obtaining a spectrogram of the meteor.

The trail was so short that no velocity determination could be obtained from the negative of the occulting-shutter camera. Since there could not be an optical velocity determination, the value of 10.4 kilometers per second from the flash X-rays of a range test at 1 atmosphere of a similar accelerator had to be used. The initial velocity of the expelled particles of the liner are not strongly dependent upon ambient air pressure for this shaped-charge accelerator. The resolved trail from the flight test was 100 meters long and its duration, calculated from the velocity, was 0.01 second. The light curve, or plot of the variation of light intensity of the artificial meteor with the distance along the trail for panchromatic film is presented in figure 9. The light intensity is extrapolated

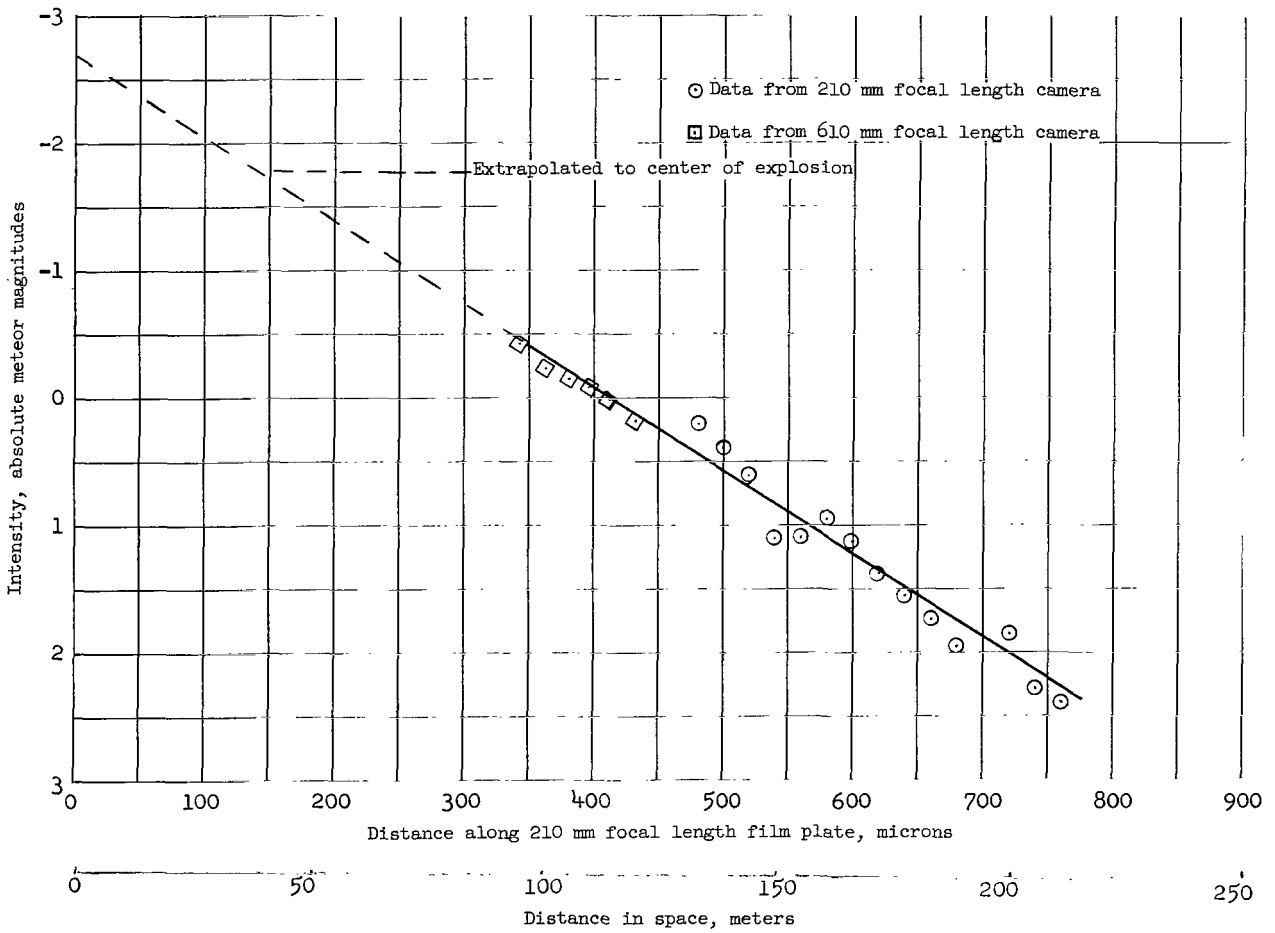

Figure 9.- Light curve of artificial meteor for panchromatic film.

back to the origin of the explosion and is plotted in absolute meteor magnitudes as a function of distance along the trail in space and as a function of distance on the film. The detected maximum of the radiation trail was -0.4 of an absolute meteor magnitude.

The shape of the light curve is substantiated by the experimental and theoretical results presented in reference 5, and by the results of relative photometry performed upon the spatially resolved lines of 4272, 4308, 4326, 4384, 4405, and 4415 angstroms of the spectrogram of the event. Both the experimental light curve for an artificial aluminum dust-ball meteor and a theoretically predicted light curve based upon a constant particle size are nearly straight-line monotonically decreasing functions of distance. Light curves for spatially resolved prominent iron lines of the meteor spectrum are presented in figure 10. The ordinate of the relative light curves was determined by taking

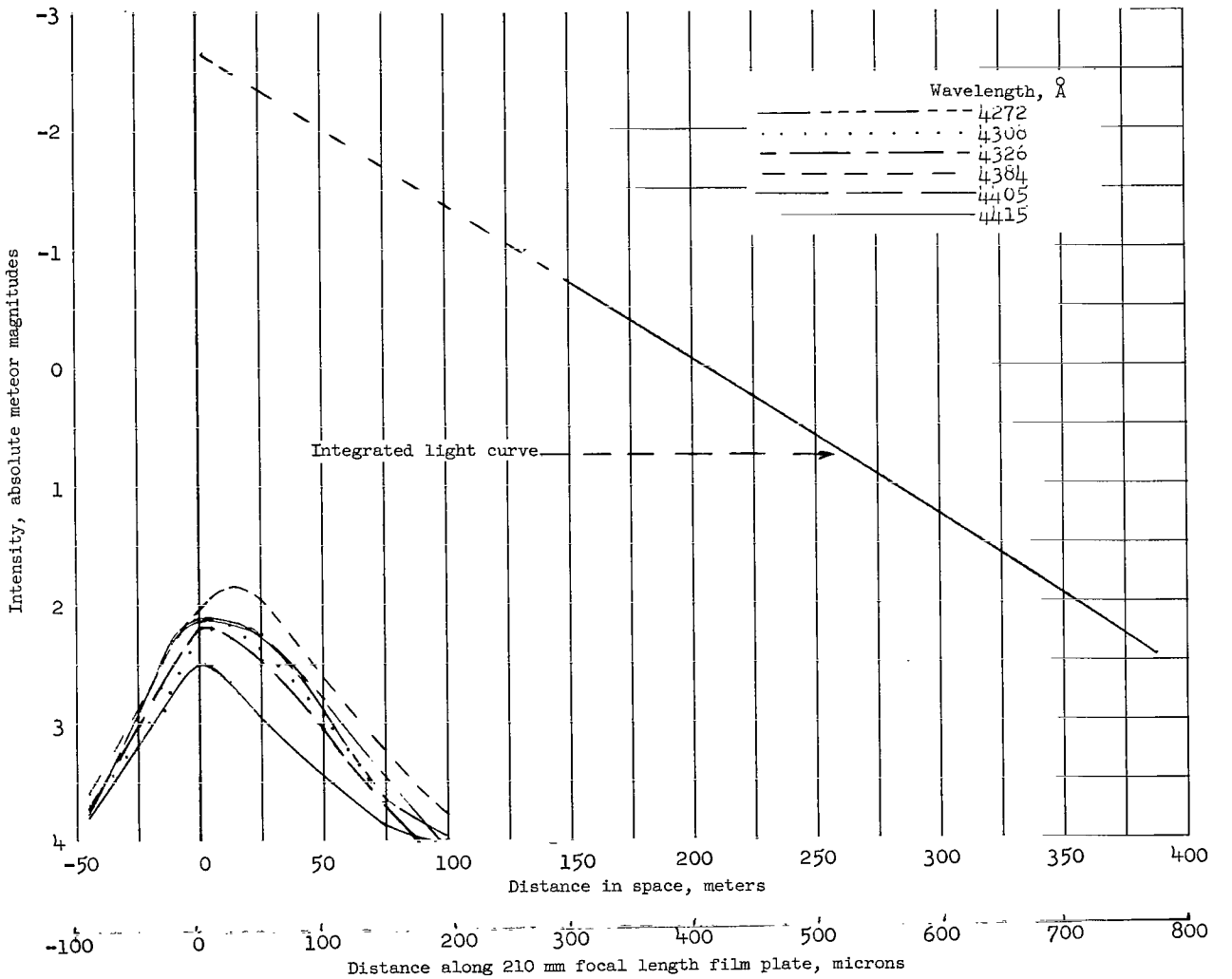

Figure 10.- Light curves for resolved prominent iron lines.

the ratio of the intensities of these lines in an arc spectrum to the integrated intensity of all iron lines in an arc spectrum in the wavelength range 3750 angstroms to 5600 angstroms. This relation was used because of the similarity between the meteor spectrum and the iron arc spectrum shown in figure 11. The relative light-curve data indicate that the spectrally undispersed light curve probably had a steeper slope near the origin than the extrapolated light curve of figure 9. Hence, a value of τ obtained from the extrapolated light curve represents a conservative value, that is, a lower limit of τ for this experiment. No information on particle size, other than that the particles are macroparticles, is available. However, since the mean free path at 47 kilometers is approximately 60 microns, it is believed possible that most of the particles experienced the same flow conditions that they would have experienced if the event had occurred at a natural meteor height of 70 kilometers. However, because this meteor did not occur at a natural meteor height, because no optical velocity measurements were made, and because 87 percent of the total light is based upon the extrapolated part of the light curve, the value of τ obtained from the extrapolated light curve should be used with caution, even as a lower limit.

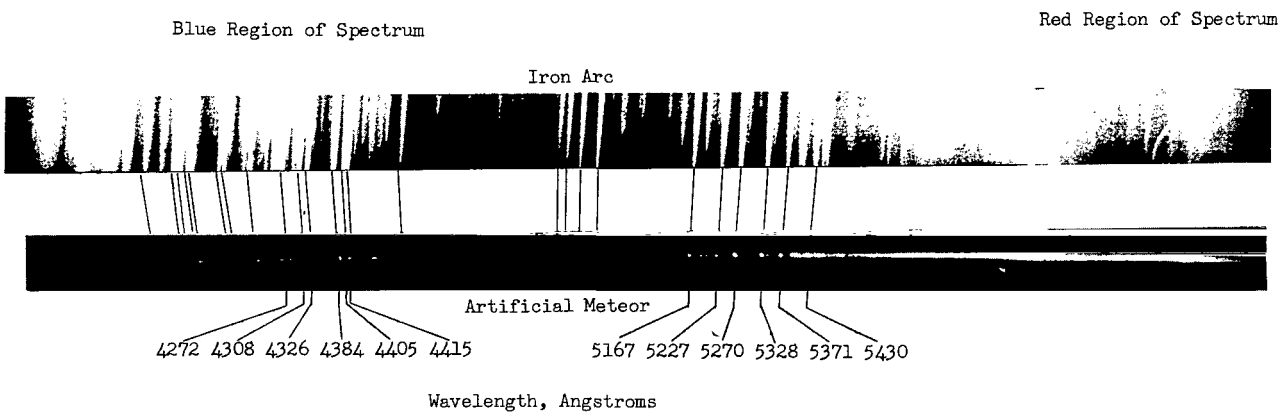

Figure 11.- Enlargements of iron-arc spectrogram and artificial meteor spectrogram.

If all of the mass is assumed to be consumed and the velocity is assumed constant for the life of the meteor, equation (2) can be rewritten as:

$$\sum_{1}^{N} I_n \Delta t_n = + \frac{1}{2} \tau m V^2 \tag{5}$$

or

$$\tau = \frac{2}{mV^2} \sum_{1}^{N} I_n \Delta t_n \tag{6}$$

The minus sign of equation (2) has disappeared because dm/dt is negative in equation (2) but both m and Δt are taken as positive quantities in the above expressions. The value of I_n is obtained from the light curve of figure 9 by using the equation

$$\log I = 9.90 - 0.4m \tag{7}$$

A value of τ for panchromatic film of 0.95×10^{-3} is obtained by using values of $m = 1.5$ grams, $V = 10.4$ kilometers per second, and Δt intervals of 0.001 second. A reciprocity failure-corrected value of τ for panchromatic film of 2.5×10^{-3} is obtained for a 2-gram stainless-steel simulated compact meteor from reference 4. The τ obtained from this dust-ball meteor can be compared crudely with a value of τ predicted by Öpik's theory of reference 1. A value of τ of 0.72×10^{-3} for visual observation is obtained from reference 1. A color correction is necessary to convert τ for panchromatic film to τ for visual observations. Using a color index of 2.8 magnitudes gives a value of 0.72×10^{-4} for a lower limit of τ for visual observation for this experiment. This value of τ is smaller by a factor of 10 than the value of τ predicted by Öpik's theory for an iron dust-ball meteor of this same mass and velocity. A derivation of equation (7) and a comprehensive discussion of color indexes can be found in reference 3.

An enlargement of the spectrum of the event is presented as figure 11. From the evaluation of this photograph, the densitometer tracing of the spectrum of figure 12, and the composition of the shaped-charge accelerator, it is believed that the meteor trail was primarily blue as a result of the prominent iron lines at 4272, 4308, 4326, 4384, and 4405 angstroms, and that the light in the red region of the spectrum is mostly from the detonation of the charge but does contain a contribution of iron oxide radiation from the meteor. Although only the 11 prominent iron lines could be spatially resolved, approximately 200 lines from more than 35 multiplets of iron have been identified in a wavelength reduction of the spectrum. A trace of the cast-iron liner impurity manganese was observed. The absence of the aluminum lines at 3944 and 3961 angstroms confirms that the meteor trail was produced by the iron dust-ball particles and not by the aluminum case of the shaped-charge accelerator. The absence of the sodium D lines, which are present in a large number of natural meteor spectra, is noted.

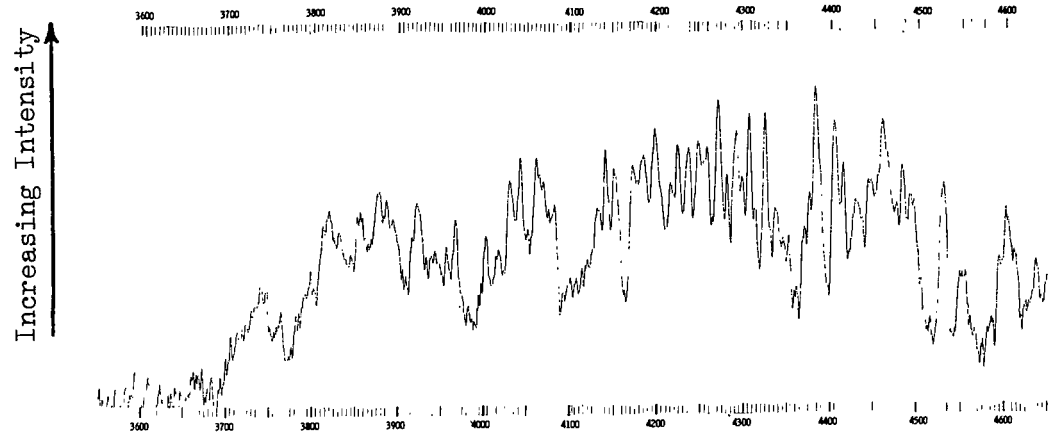

(a) 3550 to 4650 angstroms.

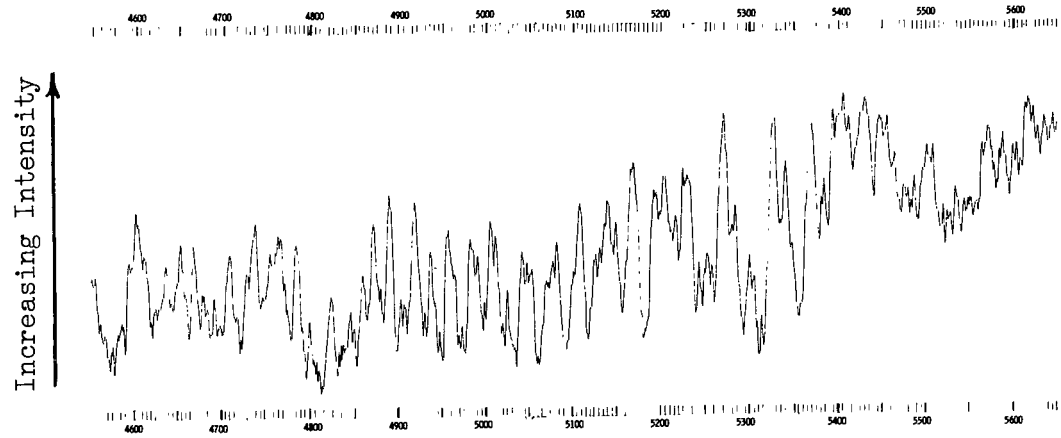

(b) 4550 to 5650 angstroms.

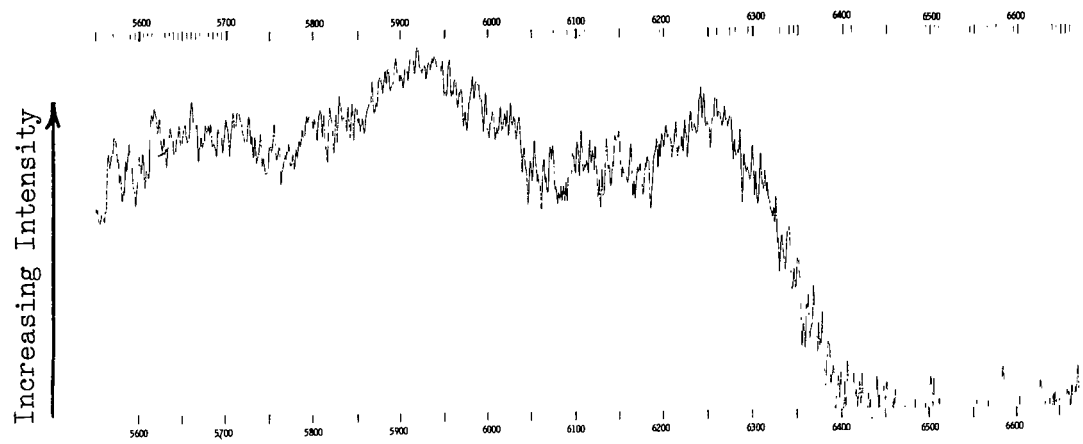

(c) 5550 to 6650 angstroms.

Figure 12.- Densitometer tracing of meteor spectrum. Intensities are relative.

CONCLUSIONS

The following conclusions were drawn from the optical measurement of a 1.5 gram, 10-kilometer-per-second, artificial low-density iron meteor at an altitude of 48 kilometers:

1. The shaped-charge accelerator performed satisfactorily under flight conditions. The aluminum case did not contaminate the meteor.

2. The optical instrumentation used is capable of recording the artificial meteors produced by this method at natural meteor altitudes (70 km).

3. The value of panchromatic luminous efficiency for the low-density iron meteor, $\tau = 0.95 \times 10^{-3}$, is heavily weighted by the extrapolated part of the light curve of the meteor and should be used with caution, even as a lower limit.

Langley Research Center,
National Aeronautics and Space Administration,
Langley Station, Hampton, Va., February 4, 1966.

REFERENCES

1. Öpik, Ernst J.: Physics of Meteor Flight in the Atmosphere. Interscience Publ., Inc. (New York), 1958, p. 147.

2. McKinley, D. W. R.: Meteor Science and Engineering. McGraw-Hill Book Co., Inc., 1961.

3. Ayers, Wendell G.: Luminous Efficiency of an Artificial Meteor at 11.9 Kilometers per Second. NASA TN D-2931, 1965.

4. Jewell, W. O.; and Wineman, A. R.: Preliminary Analysis of a Simulated Meteor Reentry at 9.8 Kilometers per Second. NASA TN D-2268, 1964.

5. McCrosky, Richard E.: Observations of Simulated Meteors. Smithsonian Contributions to Astrophysics, vol. 5, no. 4, 1961, pp. 29-36.

6. Whipple, Fred L.: A Comet Model. I. The Acceleration of Comet Encke. The Astrophysical Jour., vol. 111, Mar. 1950, pp. 375-394.

7. Boss, Benjamin: General Catalogue of 33342 Stars for the Epoch 1950. Pub. No. 468, Vol. III, Carnegie Inst. of Washington, 1937.

8. Cook, Allan F.; and Millman, Peter M.: Photometric Analysis of a Spectrogram of a Perseid Meteor. Astrophys. J., vol. 121, no. 1, Jan. 1955, pp. 250-270.

9. Whipple, Fred L.; and Jacchia, Luigi G.: Reduction Methods for Photographic Meteor Trails. Smithsonian Contributions to Astrophysics, vol. 1, no. 2, 1957, pp. 183-206.

10. Gatterer, A.; and Junkes, J.: Atlas der Restlinien. I. Band – Spektren von 30 Chemischen Elementen. 2. Auflage. Specola Vaticana (Città del Vaticano), 1947.

11. Harrison, George R., compiler: Massachusetts Institute of Technology Wavelength Tables. John Wiley & Sons, Inc., 1956.

12. Anon.: U.S. Standard Atmosphere, 1962. NASA, U.S. Air Force, and U.S. Weather Bureau, Dec. 1962.

"The aeronautical and space activities of the United States shall be conducted so as to contribute . . . to the expansion of human knowledge of phenomena in the atmosphere and space. The Administration shall provide for the widest practicable and appropriate dissemination of information concerning its activities and the results thereof."

—NATIONAL AERONAUTICS AND SPACE ACT OF 1958

NASA SCIENTIFIC AND TECHNICAL PUBLICATIONS

TECHNICAL REPORTS: Scientific and technical information considered important, complete, and a lasting contribution to existing knowledge.

TECHNICAL NOTES: Information less broad in scope but nevertheless of importance as a contribution to existing knowledge.

TECHNICAL MEMORANDUMS: Information receiving limited distribution because of preliminary data, security classification, or other reasons.

CONTRACTOR REPORTS: Technical information generated in connection with a NASA contract or grant and released under NASA auspices.

TECHNICAL TRANSLATIONS: Information published in a foreign language considered to merit NASA distribution in English.

TECHNICAL REPRINTS: Information derived from NASA activities and initially published in the form of journal articles.

SPECIAL PUBLICATIONS: Information derived from or of value to NASA activities but not necessarily reporting the results of individual NASA-programmed scientific efforts. Publications include conference proceedings, monographs, data compilations, handbooks, sourcebooks, and special bibliographies.

Details on the availability of these publications may be obtained from:

SCIENTIFIC AND TECHNICAL INFORMATION DIVISION

NATIONAL AERONAUTICS AND SPACE ADMINISTRATION

Washington, D.C. 20546